An *In Vitro* Model for Retinal Laser Damage[‡]

Michael L. Denton[a], Michael S. Foltz[a], Kurt J. Schuster[a], Larry E. Estlack[b], Harvey M. Hodnett[a], Gary D. Noojin[a], and Robert J. Thomas[c]

[a]Northrop Grumman, Warfighter Concepts and Applications Department, San Antonio, TX, USA, 78228-1330
[b]Conceptual MindWorks, Inc., San Antonio, TX, USA, 78228
[c]Air Force Research Laboratory, AFRL/HEDO, Brooks City-Base, TX, USA, 78235-5214

ABSTRACT

Ocular laser exposures resulting in damage at the retina typically involve cellular alterations in the retinal pigment epithelial (RPE) layer. To provide guidelines for eye-safe exposure to lasers, the laser safety community has relied on damage assessment in nonhuman primate studies. Simple and reliable model systems for laser bioeffects that use cultured RPE cells, rather than animals, are thus desirable. We have characterized our artificially pigmented hTERT-RPE1 model by identifying ED_{50} thresholds over a wide range of laser parameters and cell culture conditions. When summarized as action spectra and temporal action profiles (log threshold fluence versus log exposure duration), trends (pigment-dependent) in our cell model data are strikingly similar to the threshold trends reported for animal models (literature). In addition, the rapidity and flexibility (laser delivery) with which studies are performed in our culture model has benefited computational modeling efforts.

Keywords: laser, threshold, action spectra, temporal action profile, RPE cell, pigmentation, model, Probit

INTRODUCTION

Results of *in vivo* studies have shown that laser damage in the retina depends upon wavelength, power density, and duration of the exposure.[1-3] Damage assessment has been in the form of a minimum power density leading to a visible lesion,[1,4] or as a statistical evaluation of binary (yes or no) assignments relative to a wide range of power densities bracketing the threshold using the Probit method.[5,6] Output from the Probit analysis is a correlation between laser dose and the probability of achieving a damaging event in the future, given the same laser parameters. An estimated dose (ED) for damage can be described for a specific exposure in laser bioeffects research in much the same way as for a cytotoxic chemical in the field of toxicology. Thus for laser studies, an ED_{50} value is the laser dose predicted to produce a lesion 50% of the time for a given set of laser exposure conditions. Threshold values like the ED_{50} provide a measure of the efficiency of a laser exposure condition to produce a lesion. An action spectrum is useful in comparing the efficiency of laser damage in a wavelength-dependent fashion. Comparison on log-log axes of threshold fluences with their respective exposure durations (termed here as temporal action profile) can provide insight into damage mechanisms. These same analyses can be used to characterize *in vitro* models for laser damage.

Current doctrine describes three types of laser damage mechanisms in the cells and tissues of animals.[7] Photomechanical damage occurs when sufficient laser energy is deposited in pulses of about 5 - 50 μs and shorter, leading to instantaneous cellular damage from acoustic shock-waves and localized steam around absorbing particles.[8-10] At longer laser pulse durations, and in contrast to photomechanical mechanisms, thermal diffusion away from the absorbing particles is more gradual. Cell damage from this photothermal

[‡] Opinions, interpretations, conclusions, and recommendations are those of the authors and are not necessarily endorsed by the United States Air Force.

Optical Interactions with Tissue and Cells XVIII, edited by Steven L. Jacques, William P. Roach, Proc. of SPIE Vol. 6435, 643515, (2007) · 1605-7422/07/$18 · doi: 10.1117/12.701067

mechanism[11-13] is due to denaturation of intracellular macromolecules rather than from physical expansions. Over the years, there have been theoretical models developed to describe photothermal damage,[14-18] and the *in vivo* threshold data has played a vital role in validating these models. Finally, with a combination of shorter wavelengths (blue and ultraviolet) and longer exposure durations (around 10 s and longer), photochemical mechanisms[19-23] come into play, especially cellular oxidation. Currently, there are no computer modeling and simulation programs that accurately predict photochemical damage.

There undoubtedly exist exposure conditions whereby both photothermal and photochemical mechanisms, in varying degrees, contribute to the damage of cells. Although observable trends seen in the action spectra and temporal action profile in ocular studies can provide clues regarding mechanisms of lesion formation, and histopathologic analysis pinpoints which cells are involved, molecular techniques are required to study the metabolic mechanisms of laser damage. Even with the advent of laser-capture microdissection, the prospect of biochemically analyzing sufficient biomaterial of a retinal minimum visible lesion (MVL) generated by a laser exposure is an arduous task. Certainly, understanding the biochemical changes associated with both photothermal and photochemical damage by laser exposure would give insight into protection, prevention and treatment modalities, but it would also benefit computer modeling efforts.

In our previous work,[24-27] we have described our artificially pigmented retinal pigment epithelial (RPE) cell system, showing how overall pigmentation can be varied by adding different numbers of isolated melanosome particles (MPs) to cells in culture (Figure 1).

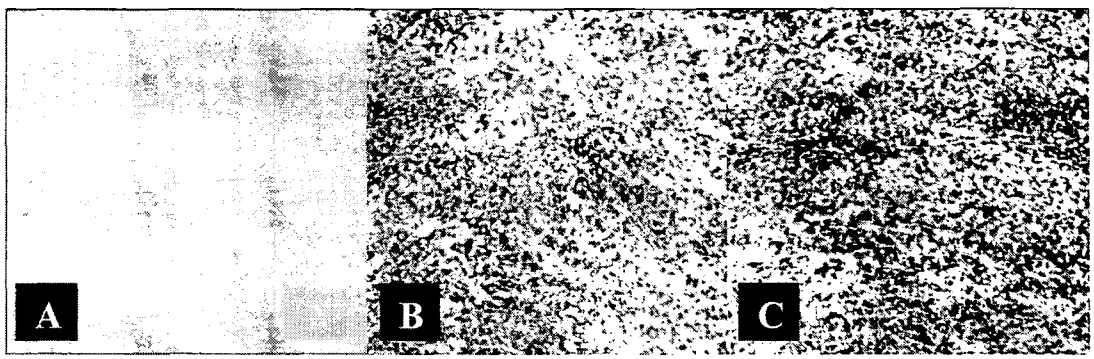

Figure 1. Confluent hTERT-RPE1 cells in cultures (35-mm dishes) to which 40 µl (panel B) and 100 µl (panel C) isolated bovine melanosomes were added. Confluent hTERT-RPE1 cells to which no melanosomes were added are shown in panel A. Photos for all three panels were taken through the 10x objective of an inverted microscope. (Taken from reference 26).

The number of melanosomes added to the cultured RPE cells linearly affects the bulk absorption coefficient of the cell monolayers for a given wavelength (Figure 2). The ability to vary pigmentation, and thus absorption properties of the RPE cells can be used as a valuable tool for studying the role of pigmentation in laser-tissue interactions.

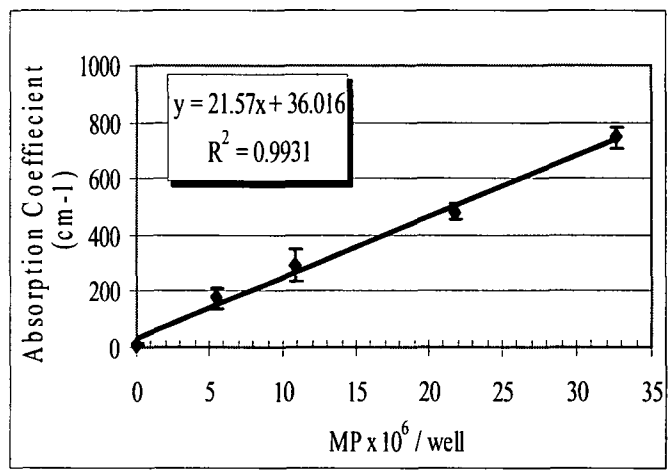

Figure 2. Linear response of bulk absorption coefficient (460 nm) with respect to the number of melanosomes added to the RPE cells (Taken from reference 25).

We have also described the fluorescent cytotoxicity assay used as our damage endpoint in our *in vitro* model system (Figure 3). The method, which actually indicates the integrity of the plasmalemma, provides a qualitative product useful for identifying acute damage.

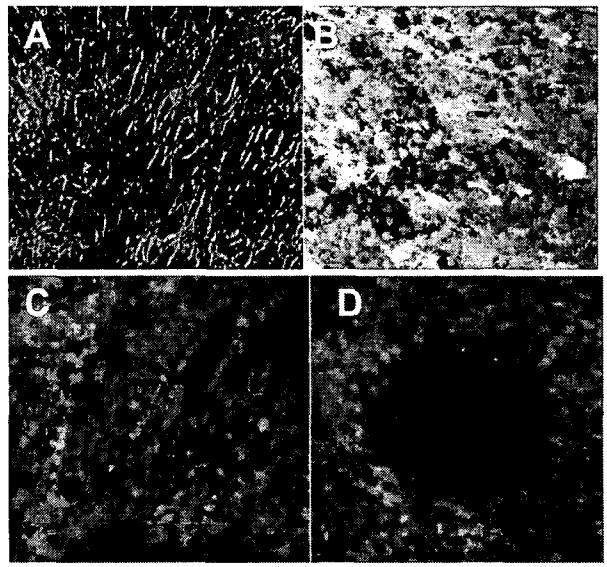

Figure 3. Confluent hTERT-RPE1 cell cultures that have no melanosomes added (panel A) or 60 melanosomes per cell added (panel B). The pictures shown are the result of overlaying three photos per microscopic field of view; bright-field, emission of calcein, and emission of the ethidium homodimer. Photos in panels C and D, which do not have the bright-field overlay, provide examples of artificially pigmented cells without (C) and with (D) laser-induced damage. Photos were taken through the 20x objective of an inverted microscope. (Taken from reference 26)

Finally, we have continued to improve our ability to control the environmental conditions during laser exposures, especially for extended durations leading to photochemical damage.[24] Here, the *in vitro* system was shown to be useful for comparing how melanin, laser mode (mode-locked or CW), and antioxidants, effect photochemical damage to the cells. However, our predictive modeling for the thermal response to the cells was not accurate, and we are currently taking steps to correct this.

The present work is a comparison of damage thresholds across four wavelengths and two densities of melanosomes within the RPE cells. We show that, although the absolute values of the thresholds differ from MVL data taken from the literature, we see trends in the action spectra and temporal action profiles that are consistent with that from ocular exposures in rhesus monkeys. This is a major validation of the *in vitro* model, and a starting point for both refining existing computer models and identifying interesting laser exposure conditions to study at the molecular level.

METHODS

2.1 Cell culture and damage assessment.

Stock cultures of hTERT-RPE1, a human-derived retinal pigment epithelial cell line (BD Biosciences ClonTech Labs, Palo Alto, CA), were maintained at standard growth conditions (37 °C; 95:5 air:CO_2) using 1:1 DMEM/F12 media containing 10% fetal bovine serum, antibiotics, and 10 mM HEPES buffer (pH 7.4). Cells used in laser exposure experiments were seeded in 96-well plates at 27000 cells per well, pigmented the following day with isolated bovine MPs,[28] and exposed (or used as controls) on the second day post-seed. Adhering to this schedule (seed wells with cells, add melanosomes, and expose to laser, each on consecutive days) provided monolayers with consistent cell density with >95% viability. No residual MPs were found in growth medium after incubation with the RPE cells. This led to our conclusion that there were approximately 10-fold more intracellular melanosomes after incubation with stock volumes equivalent to 1600 MP/cell compared to 160 MP/cell.

Cells were exposed to lasers with 200 µL Hank's Balanced Salt Solution (HBSS) in each well. After exposure to lasers, this HBSS was replaced with complete growth medium and the cells were placed at standard growth conditions for 1 hr. Finally, cells were assayed for viability using 1.7 µM calcein-AM and 1.4 µM Ethidium homodimer 1 (EthD1) in 0.1 mL HBSS (10 min at 37 °C). Exposure sites within wells

were identified as positively stained when nuclei were fluorescent with EthD1 (bandpass exciter of 475-545 nm and a barrier filter at 590 nm) and as a region devoid of staining by calcein-AM (bandpass exciter of 460-490 nm and a bandpass emitter of 490-530 nm). Scoring of damage by three individuals was blind of dosimetry, and a score (yes/no) for damage required a consensus from two. These binary data were input into the Probit software package.[6] In addition to probability-dose information (ED_{50}), the Probit output includes uncertainty intervals (fiducial limits at 95% confidence) related to the ED value, and the Probit slope (δ probability $\div$ δ dose, at a probability of 0.5 for ED_{50}).

2.2 Lasers, beam delivery, and cell exposures.

Three different lasers provided the four wavelengths used in our study. A large-frame Krypton laser (Saber-08W-K, Coherent) was used for its 413-nm line. The 514-nm and 458-nm exposures were delivered from a large-frame Argon laser (Innova 200, Coherent). A diode-pumped ND:YVO4 laser (Millennia Xs, Spectra Physics), with intracavity doubling, was used for the 532-nm exposures. Verification of laser wavelength was performed with a spectrometer (Ocean Optics).

Figure 4 provides a schematic representation of the laser delivery to cells in 96-well plates. Attenuation of laser power was achieved by the combination of a half-wave plate ($\lambda/2$) and polarizing beam splitter (Pol). All beams were then co-aligned to a common optical path using apertures and a flip-up mirror (F). The optical path included a telescope (T), a beam shaper (BSh, model GBS-AR14, Newport), a computer-controlled shutter (S), and a single lens (L) imaging system generating a beam diameter of about 0.3 mm (88-mm FL lens) at the cells. The telescope allowed for collimated beam expansion to 4.7 mm prior to entry into the beam shaper, which converted the beam to a flat-top profile. The imaging system was designed to image the beam at the near-field output of the beam shaper (about 8 mm diameter) via 0.05 x magnification. For consistent spot sizes and cleaner flat-top profiles, the beam was passed through an aperture to provide the desired diameter. The effect of the column of HBSS above the cells during exposure was taken into account when determining laser beam diameter (knife-edge method).

Cells were systematically exposed to laser irradiation for time intervals between 0.1 s and 100 s at irradiance ranges useful for determining viability thresholds. The 96-well plates were suspended (without lids) in the beam path using a specialized holder attached to x-y translational stages equipped with computer-controlled motors. Ambient temperatures during experiments ranged from 18 °C – 25 °C.

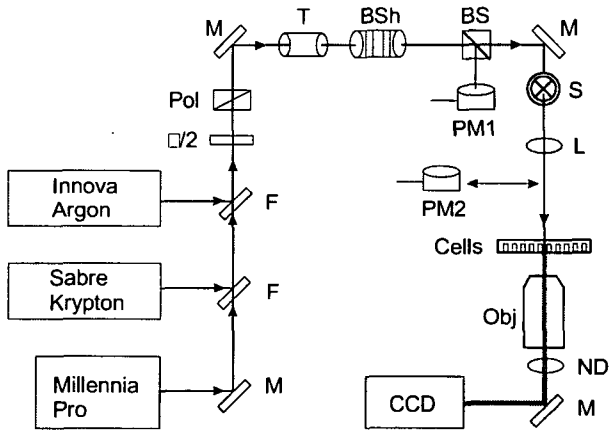

Figure 4. Beam Delivery. M, mirror; F, flip-up mirror; Pol, polarizing cube; T, optical telescope; BSh, beam shaper; S, shutter; L, lens; PM, power meter; ND, neutral density filter; CCD, charge-coupled device camera; Obj, microscope objective.

RESULTS

Figure 5 shows fluorescence (panels A and C) and bright field (panels B and D) images for each of the two levels of pigmentation in our hTERT-RPE1 cells. As expected, there was substantially more pigmentation distributed throughout the monolayer when adding more melanosomes. Because we saw no residual MPs after the phagocytosis period we expect the two levels of pigmentation to be about 10 fold different. Also note that there was sufficient calcein-AM dye in the cells containing the high density of MPs to assay for damage.

Threshold (ED_{50}) values were obtained for exposure to 532 nm, 514 nm, 458 nm, and 413 nm for 0.1 s, 1.0 s, 10 s, and 100 s durations each, in hTERT-RPE1 cells containing about 160 MP/cell. Additionally, ED_{50}

values for exposure to 532 nm, 514 nm and 458 nm for 1 s, 10 s, and 100 s durations each were obtained in RPE cells containing about 1600 MP/cell. The number of laser exposures used in each individual ED_{50} study ranged from 20 to 100, where the total number of exposures used in this study was 1,265. The 95% fiducial limits (FLs) for the 160 MP/cell data sets ranged from 3% - 40% from their respective ED_{50} value (average variance of 17% with SD of 9%). The 95% FLs for the 1600 MP/cell data sets ranged from 7% - 25% from their respective ED_{50} value (average variance of 16% with SD of 4%).

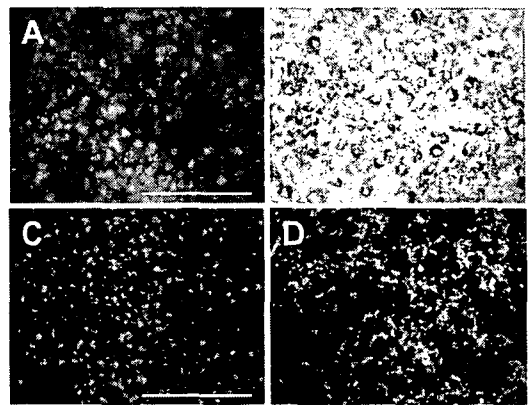

Figure 5. Microscopic assessment of two levels of pigmentation in hTERT-RPE1 cells. Panels A and B: 160 MP/cell. Panels C and D: 1600 MP/cell.

Our complete *in vitro* threshold study is summarized as irradiance action spectra (Figure 6) and fluence action spectra (Figure 7). It is apparent from both types of analysis that there was a pigment dependent effect on the trends for the data. The irradiance action spectra for the 160 MP/cell show a substantial increase in sensitivity (larger inverse irradiance value) for cells exposed for 100 s at 413 nm relative to the other wavelengths and exposure durations. Although not perceptible on this plot (Figure 6), there was a trend of increasing sensitivity as wavelength was shortened, and as exposure duration was lengthened at the 160 MP/cell pigmentation. However, these trends completely broke down for cells having more pigmentation (see inset).

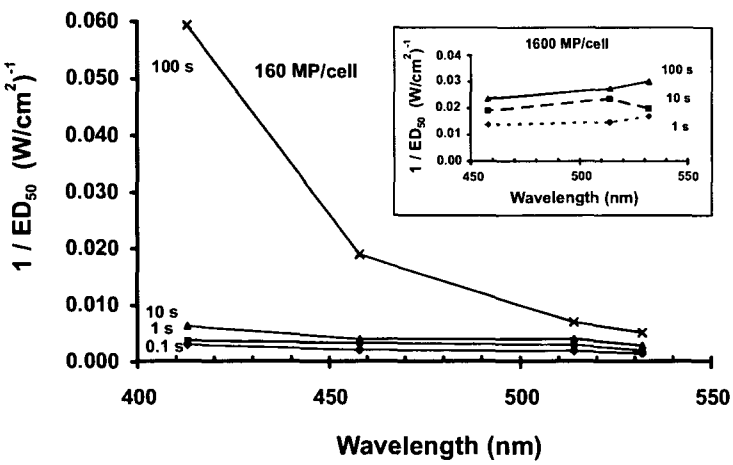

Figure 6. Irradiance action spectra for all laser exposure conditions for cells containing about 160 MP/cell. Inset provides data for cells having an equivalent to 1600 MP/cell. Note that the unit for the ordinate is inverse irradiance.

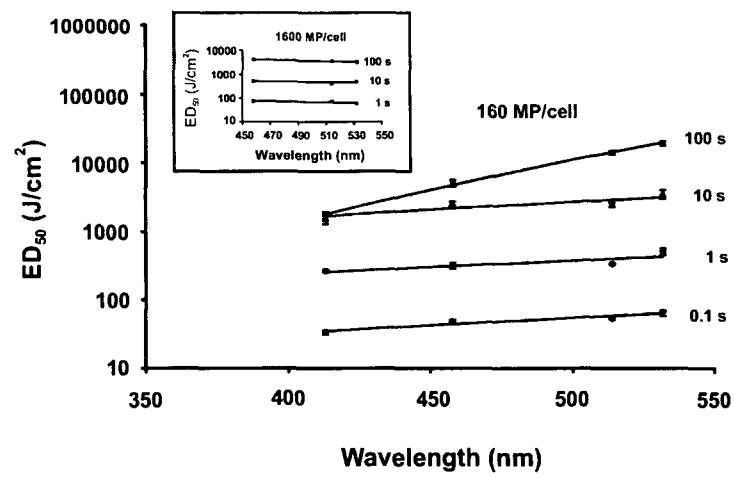

Figure 7. Fluence action spectra for all laser exposure conditions for cells containing about 160 MP/cell. Inset provides data for cells having an equivalent to 1600 MP/cell. Note the semi-log plot.

Expressing the action spectra with fluence (Figure 7) has the advantage of indicating irradiance reciprocity (notice that the thresholds for 413 nm 10 s and 100 s overlap on the graph) and exposure conditions with combined damage mechanisms. Note that each of the spectra for 0.1 s, 1.0 s, and 10 s all have a slight slope (function of $\lambda^{2.3}$ on average), indicative of increased cellular sensitivity at the shorter wavelengths for what is presumed to be essentially purely photothermal damage. The slope of the line for the 100 s exposures is steeper ($\lambda^{9.5}$), indicating the greater wavelength dependence of cell damage as more photochemical effects become apparent. The graphic depiction shown (Figure 7) implies that by holding exposure duration at 100 s, damage will proceed by purely photothermal (532 nm), purely photochemical (413 nm), and by varying combinations of photothermal and photochemical (514 nm and 458 nm) mechanisms by simply adjusting the laser wavelength. It is notable that the equations describing the data from exposures to the highly pigmented cells (inset to Figure 3) have negative slopes.

Figure 8 relates our *in vitro* damage thresholds (fluence) to exposure duration for each of the wavelengths using temporal action profiles. The data point for the 3600-s exposure at 458 nm is taken from our previous article[24]. Solid lines represent data from exposures to cells having 160 MP/cell while dashed lines represent data from the cells with higher MP density. The solid lines for 532-nm and 413-nm data are fairly well separated, but those of the 514-nm and 458-nm essentially overlap for the three shortest time points. There was no distinction between any of the dashed lines at any of the time points.

For the blue laser wavelengths, the threshold data level off somewhere between 10 s (458 nm) and 20 s (413 nm). This leveling off in fluence thresholds for both 458 nm and 413 nm at the longer exposures is indicative of the principle of reciprocity, where photochemical damage mechanisms prevail. There was no reciprocity (up to 100 s exposures) for damage to cells with the high MP density.

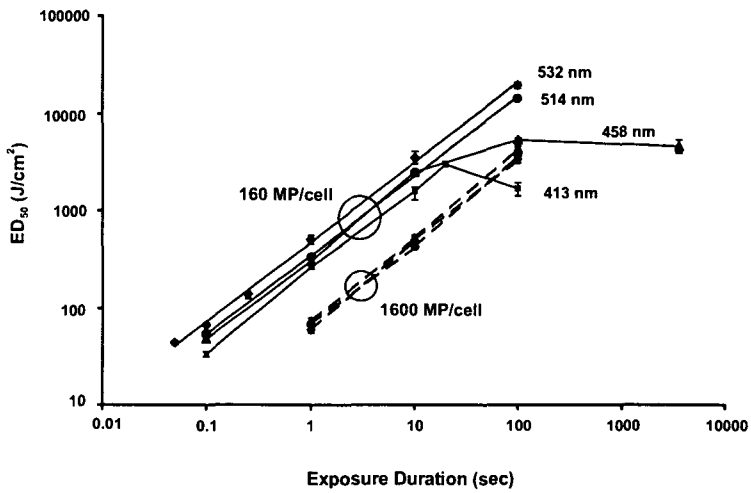

Figure 8. Temporal action profiles for all laser exposure conditions for cells containing about 160 MP/cell and 1600 MP/cell.

DISCUSSION

Devising an *in vitro* physical model (cells, tissues, explants, etc) for laser damage to the eye or skin that accurately predicts *in vivo* thresholds is challenging. The immediate surroundings of target cells in the animal make each tissue unique. Some factors involved in dosimetry requirements for damage *in vivo* include the optical properties (wavelength-specific) of all tissues preceding the target cells, tissue blood flow, and varying endpoints for damage assessment. At the cellular level, the differentiated state of a cell dictates its metabolic status, which influences both its susceptibility to damage and its potential for recovery. A good example of this is the RPE cell. Due to their environment and cellular functions, RPE cells are subjected to oxidative stress (high oxygen tension) and may undergo a form of protective adaptive response over time. However, age also increases the abundance of lipofuscin, which has been implicated in oxidative pathology.[29-31] Isolation methods are available for melanosome and lipofuscin particles which have enabled some variability in physical models. Nevertheless, we contend that the utility of an *in vitro*

physical model is reliant upon its simplicity rather than it being an exact replica of the *in vivo* condition, which is complex and variable.

Unlike the physical models, computational models (also *in vitro*) should have accurate predictive capabilities with *in vivo* threshold values being the standard for evaluation. As such, these predictive models could have a role in establishing laser safety standards. However, refinement of such models is not easy and it is not ethically acceptable to perform large numbers of laser damage studies in animals just to test theoretical principles. Reliable data taken from an *in vitro* physical model could prove useful in refining computational models for laser damage, especially if they mimic basic threshold trends from animal studies. We show in this report that our physical *in vitro* RPE system, at roughly 160 MPs/cell, follows the same general trends for damage thresholds seen in the Rhesus animal model.

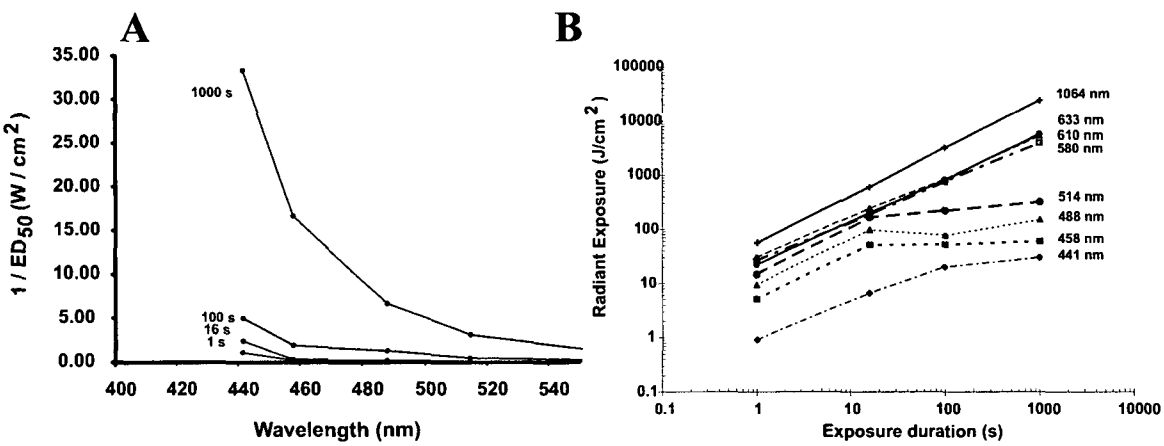

Figure 9. *In vivo* irradiance action spectra (A) and temporal action profiles (B) for threshold data taken from Ham et al.[2]

Figure 9 provides the animal data for comparison with our *in vitro* system. Notice the increasing sensitivity of the Rhesus retina at the shorter wavelengths, and for the longer exposure durations within a given wavelength (panel A). The temporal action profiles in Figure 9B show the leveling off of fluence (irradiance reciprocity) at around 10 s for the shorter wavelengths, which was the same point of transition seen in Figure 8. One difference in Figures 8 and 9B is for the exposures to 514 nm. The *in vitro* system indicates no reciprocity, but it is evident in the *in vivo* system. This can be explained by examining the differences in the time of damage assessment. Our cell culture system stains for damage at 1 hr post exposure while Ham et al. waited 48 hr post exposure before looking for MVLs. Gibbons and Allen,[32] studied MVL damage to exposure to 514 nm in the Rhesus at both 1 hr and 24 hr post exposure. This group found a continuing straight line (log-log plot) for the 1 hr temporal action profile (like our *in vitro* results), and a transition to reciprocity for the 24 hr profile. If one compares the actual threshold values for the plots in Figures 6 – 9 it is apparent that the *in vitro* values are larger. By increasing the pigmentation 10 fold in our RPE cells, the damage thresholds were reduced (cells were more sensitive), but the trends in the data were lost leaving a less than desirable model system. As discussed previously, the disparities between *in vitro* and *in vivo* thresholds can be attributed to differences in spot size and time of damage assessment. In fact, the threshold values reported by Gibbons and Allen (Probit ED_{50}) also differ substantially from Ham et al. (minimum irradiance generating a lesion).

By focusing on the similarities in damage trends in the cell and animal models, we confirm that the transition from photothermal to photochemical damage mechanisms occur at the same wavelengths (514 nm is a pivotal wavelength) and exposure durations (10 s is pivotal) for both cell (pigment dependent) and animal models. With this validation, our RPE cell model can be used to study other effects of

pigmentation, lipofuscin, and a host of other environmental factors as they relate to this baseline response behavior. Various cellular responses to laser exposure, such as oxidation, spot size dependence, effects of aqueous interfaces, exact inflections between damage mechanisms, and molecular profiling (transcriptomics and proteomics), are more easily measured and studied in the cell model. Using our *in vitro* data, we are beginning to incorporate photochemical rate processes into traditional thermal models in the hopes of generating a universal model for laser damage predictions.

REFERENCES

1. W.T. Ham, Jr, J.J. Ruffolo Jr, H. Mueller, and D. Guerry III, "The nature of retinal radiation damage: Dependence on wavelength, power level and exposure time," *Vision Res* .**20**, 1105-1111 (1980).
2. W.T. Ham Jr, H.A. Mueller, M.J. Ruffolo Jr, and A.M. Clarke, "Sensitivity of the retina to radiation damage as a function of wavelength," *Photochem Photobiol.* **29**, 735-743 (1979).
3. W.T. Ham Jr, J.J. Ruffolo Jr, H.A. Mueller, A.M. Clarke, and M.E. Moon, "Histologic analysis of photochemical lesions produced in rhesus retina by short-wavelength light." *Invest Ophthalmol Vis Sci* **17**, 1029-1035 (1978).
4. Ham WT, Mueller HA et al., "Action spectrum for retinal injury from near-ultraviolet radiation in the aphatic monkey," *Am J Ophthalmol* **93**, 299-306 (1982).
5. D.J. Finney, *Probit Analysis*. New York: Cambridge University Press: (1971).
6. C.P. Cain, G.D. Noojin, and L. Manning, "A comparison of various probit methods for analyzing yes/no data on a log scale," USAF School of Aerospace Medicine, Brooks Air Force Base, TX, USAF Technical Report AL/OE-TR-1996-0102 (1996).
7. L. Theodore, "Three major pathologic processes caused by light in the primate retina: A search for mechanisms," *Tr Am Ophth Soc* **LXXX**, 517-579 (1982).
8. Kelly MW. *Intracellular Cavitation as a Mechanism of Short-Pulse Laser Injury to the Retinal Pigment Epithelium.* Thesis. 1997; Tufts University Medford, MA.
9. R. Brinkmann, G. Huttmann, J. Rogener et al., "Origin of retinal pigment epithelium cell damage by pulsed laser irradiance in the nanosecond to microsecond time regimen," *Lasers in Surgery and Medicine* 27, 451-464 (2000).
10. Schuele G, Rumohr M, Huettmenn G, Brinkmann R. RPE damage thresholds and mechanisms for laser exposure in the microsecond-to-millisecond time regimen. *Invest Ophthalmol Vis Sci.* 2005;46:714-719.
11. Marshall, J, "Thermal and mechanical mechanisms in laser damage to the retina," *Invest Ophthalmol Vis Sci*; **9**, 97-115 (1970).
12. Welch AJ, Polhamus GD. Measurement and prediction of thermal injury in the retina of the rhesus monkey. *IEEE Transactions in Biomedical Engineering* 1984;BME-31:633.
13. Welch AJ, Van Gemert M. *Thermal Response of Tissue to Optical Radiation* New York: Plenum Press; 1995.
14. A.M. Clarke, W.J. Geeraets, and W.T. Ham, "An equilibrium thermal model for retinal injury from optical sources" *Appl. Opt.* **8**, 1051-1054 (1969).
15. Welch AJ, Priebe LA, Forster LD, Gilbert R, Lee C, Drake P. Experimental validation of thermal retinal models of damage from laser radiation. University of Texas; Contract F33615-76-C-0605 1978.
16. Torres JH, Motamedi M, Pearce JA, Welch AJ. Experimental evaluation of mathematical models for predicting the thermal response of tissue to laser irradiation. *Applied Optics* 1993;32:597-606.
17. Thomas RJ, Buffington GD, Irvin LJ, et al. Experimental and theoretical studies of broadband optical thermal damage to the retina. *Proc SPIE* 2005;5688:411-422.
18. Thomas RJ, Cain CP, Noojin GD, et al. Extension of Thermal Damage Models of the Retina to Multi-Wavelength Sources. *Proc ILSC* 2005;77-83.
19. Kremers JJM, van Norren D, "Two classes of photochemical damage of the retina," *Lasers and Light in Ophthalmology*, **2**, 41-52 (1988).

20. Stuck BE. The retina and action spectrum for photoretinitis ("blue-light hazard"). In: Matthes and Sliney Eds. *Measurements of Optical Radiation Hazards*. 1998:193-208.
21. G.A. Griess and M.F. Blankenstein, "Additivity and repair of actinic retinal lesions," *Invest Ophthalmol Vis Sci.* **20**, 803-807 (1981).
22. W.T. Ham Jr, and H.A. Mueller, "The photopathology and nature of the blue light and near-UV retinal lesions produced by lasers and other optical sources," In: Wolbarsht ed. *Laser Applications in Medicine and Biology*. New York: Plenum Publishing; 191-246 (1989).
23. W.D. Gibbons and R.G. Allen, "Retinal damage from lont-term exposure to laser radiation," *Invest Ophthalmol Vis Sci.* **16**, 521-529 (1977).
24. M.L. Denton, M.S. Foltz, L.E. Estlack, D.J. Stolarski, G.D. Noojin, R.J. Thomas, D. Eikum, and B.A. Rockwell, "Damage threshold for exposure to NIR and blue lasers in an in vitro RPE cell system," *Invest Ophthalmol Vis Sci.* **47**, 3065-3073 (2006).
25. Foltz, M.S., N.A. Whitlock, L.E. Estlack, M.A. Figueroa, R.J. Thomas, B.A. Rockwell, and M.L. Denton, "Photochemical damage from chronic 458-nm laser exposures in an artificially pigmented hTERT-RPE1 cell line," Optical Interactions with Tissue and Cells XVII, Proceedings of SPIE **6084**, 15 (2006).
26. M.L. Denton, D.M. Eikum, G.D. Noojin, D.J. Stolarski, R.J. Thomas, R.D. Glickman, B.A. Rockwell, "Pigmentation in NIR laser tissue damage," In: Laser and Noncoherent Light Ocular Effects: Epidemiology, Prevention, and Treatment, (B.E. Stuck and M. Belkin eds), SPIE **4953**, 78-84 (2003).
27. Denton, ML, D.M. Eikum, D.J. Stolarski, G.D. Noojin, R.J. Thomas, R.D. Glickman, B.A. Rockwell, "Cytotoxicity in cultured RPE: A comparative study between continuous wave and mode-locked lasers," In: Laser-Tissue Interaction XII, (S.L. Jacques, ed), SPIE **4617**, 156-160 (2002).
28. A.E. Dontsov, R.D. Glickman, and M. Ostrovsky, "Retinal pigment epithelium pigment granules stimulate the photo-oxidation of unsaturated fatty acids," Free *Radical Biol Med.* **26**, 1436-1446 (1999).
29. Cai J, Wu M, Nelson KC, Sternberg P, Jones DP, "Oxidant-induced apoptosis in cultured human retinal pigment epithelial cells", *Invest Ophthalmol Vis Sci*, **40**, 959-66, 1999.
30. Winkler BS, Boulton ME, Gottsch JD, Sternberg P, "Oxidative damage and age-related macular degeneration", *Mol Vis*, **5**, 32-42, 1999.
31. Sparrow, J. R., Nakanishi, K., Parish, C. A, "The lipofuscin fluorophore A2E mediates blue light-induced damage to retinal pigmented epithelial cells", *Invest Ophthalmol Vis Sci*, **41**, 1981-1989, 2000.
32. W.D. Gibbons and R.G. Allen, "Retinal damage from long-term exposure to laser radiation," *Invest Ophthalmol Vis Sci.* **16**, 521-529 (1977).